AIP Applied Physics Letters

Evolution mechanisms of the surface morphology of grains in ZnO thin films grown on p-InP substrates due to thermal annealing

J. M. Yuk, J. Y. Lee, Y. S. No, T. W. Kim, and W. K. Choi

Citation: Appl. Phys. Lett. 93, 021904 (2008); doi: 10.1063/1.2957467
View online: http://dx.doi.org/10.1063/1.2957467
View Table of Contents: http://apl.aip.org/resource/1/APPLAB/v93/i2
Published by the American Institute of Physics.

Additional information on Appl. Phys. Lett.

Journal Homepage: http://apl.aip.org/
Journal Information: http://apl.aip.org/about/about_the_journal
Top downloads: http://apl.aip.org/features/most_downloaded
Information for Authors: http://apl.aip.org/authors

ADVERTISEMENT

Downloaded 22 Apr 2013 to 143.248.118.122. This article is copyrighted as indicated in the abstract. Reuse of AIP content is subject to the terms at: http://apl.aip.org/about/rights_and_permissions

APPLIED PHYSICS LETTERS **93**, 021904 (2008)

Evolution mechanisms of the surface morphology of grains in ZnO thin films grown on *p*-InP substrates due to thermal annealing

J. M. Yuk,[1] J. Y. Lee,[1] Y. S. No,[2] T. W. Kim,[2,a)] and W. K. Choi[3]
[1]*Department of Materials Science and Engineering, Korea Advanced Institute of Science and Technology, Daejeon 305-701, Republic of Korea*
[2]*Advanced Semiconductor Research Center, Electronics and Computer Engineering, Hanyang University, 17 Haengdang-dong, Seongdong-gu, Seoul 133-791, Republic of Korea*
[3]*Thin Film Materials Research Center, Korea Institute of Science and Technology, Seoul 136-791, Republic of Korea*

(Received 24 March 2008; accepted 20 June 2008; published online 15 July 2008)

Transmission electron microscopy (TEM), high-resolution TEM, and atomic force microscopy images showed that the columnar structure and the surface morphology of grains in ZnO thin films grown on *p*-InP substrates were changed due to thermal treatment. The surface morphology variation of the ZnO thin films was attributed to the curvature modification of the subpopulations consisting of ZnO grains. While the top surface of the ZnO grains became parallel with the {0001} planes due to thermal treatment, the curvature of the subpopulations in the ZnO grains became rough. Evolution mechanisms of the surface morphology of ZnO thin films are described. © *2008 American Institute of Physics*. [DOI: 10.1063/1.2957467]

Recently, II-VI thin films based on wide-band-gap semiconductor compounds have attracted considerable attention because of their many potential applications in optoelectronic devices operating in the short-wavelength region.[1,2] Among these II-VI thin films, ZnO thin films are of current interest because of their potential applications in optoelectronic devices due to their large band-gap semiconductors with superior physical properties of large exciton binding energy, high optical gain, and excellent chemical stability.[3–8] Even though some works concerning ZnO thin films grown on Si substrates have been reported,[9–12] relatively few works have been performed on ZnO thin films grown on III-V compound semiconductor substrates.[13] Even though there are inherent problems due to possible cross-doping effects resulting from interdiffusion or intermixing during growth, ZnO/InP heterostructures have been particularly interesting due to the possibility of promising high-speed optoelectronic and electronic devices.[14,15] Some studies concerning the annealing effects on the ZnO films have been performed to obtain their high quality.[16] The grain growth in the polycrystalline film with a lattice mismatch in comparison with the substrate can occur due to the movement of grain boundaries, resulting in the shrinkage and elimination of small grains and in an increase in the average size of residual grains.[17] Even though some works concerning the thermal effect of ZnO grains on the surface morphology of ZnO thin films have been performed,[14–19] studies on the evolution mechanisms of the surface morphology of grains in ZnO thin films grown on *p*-InP substrates due to thermal annealing have not yet been reported.

This letter reports the evolution mechanisms of the surface morphology of grains in ZnO thin films grown on *p*-InP substrates due to thermal annealing. X-ray diffraction (XRD) measurements were carried out to investigate the effect of thermal treatment on the crystallinity of the ZnO thin films grown on *p*-InP (100) substrates. Transmission electron microscopy (TEM) and high-resolution TEM (HRTEM) measurements were carried out in order to investigate the microstructural properties of the as-grown and the annealed ZnO/*p*-InP (100) heterostructures.Atomic force microscopy (AFM) measurements were performed in order to characterize the surface roughness of the as-grown and annealed ZnO thin films.

Polycrystalline stoichiometric ZnO with a purity of 99.999% was used as a source target material. The carrier concentration of the Zn-doped *p*-InP substrates with (100) orientations used in this experiment was 1×10^{16} cm^{-3}. The InP substrates obtained from Sumitomo were alternately degreased in warm acetone and trichloroethylene (TCE) three times, etched in a Br-methanol solution, rinsed in de-ionized water thoroughly, etched in a mixture of H_2SO_4, H_2O_2, and H_2O (4:1:1) at 40 °C for 10 min, and rinsed in TCE again. After the chemically cleaned InP wafers were mounted onto a susceptor in a growth chamber, the chamber had been evacuated to 8×10^{-7} Torr. The deposition of the ZnO layer was done at a substrate temperature of 200 °C. Ar gas with a purity of 99.999% was used as the sputtering gas. Prior to ZnO growth, the surface of the ZnO target was polished using Ar^+ sputtering. The ZnO deposition was done at a radio-frequency power (radio frequency=13.26 MHz) of 100 W. The flow-rate ratio of Ar to O_2 was 2, and the growth rate was approximately 1.17 nm/min. The deposition of the ZnO layer was done at a system pressure of approximately 1×10^{-2} Torr. The thickness of the ZnO layer was 50 nm. The thermal annealing process was performed in a nitrogen atmosphere by using a tungsten-halogen lamp and was carried out for 15 min at a temperature of 400 °C.

The XRD measurements were performed by using a D/Max-RC (12 kW) diffractometer (Rigaku Co., Tokyo, Japan) with Cu Kα radiation. The TEM measurements were performed by using a Tecnai G2 F30 S-Twin field emission transmission electron microscope (FEI Co., Eindhoven, Netherlands) operating at 300 kV. The samples for the cross-sectional TEM measurements were prepared by cutting and polishing with diamond paper to a thickness of approxi-

a)Author to whom correspondence should be addressed. Electronic mail: twk@hanyang.ac.kr.

 © 2008 American Institute of Physics

Downloaded 22 Apr 2013 to 143.248.118.122. This article is copyrighted as indicated in the abstract. Reuse of AIP content is subject to the terms at: http://apl.aip.org/about/rights_and_permissions

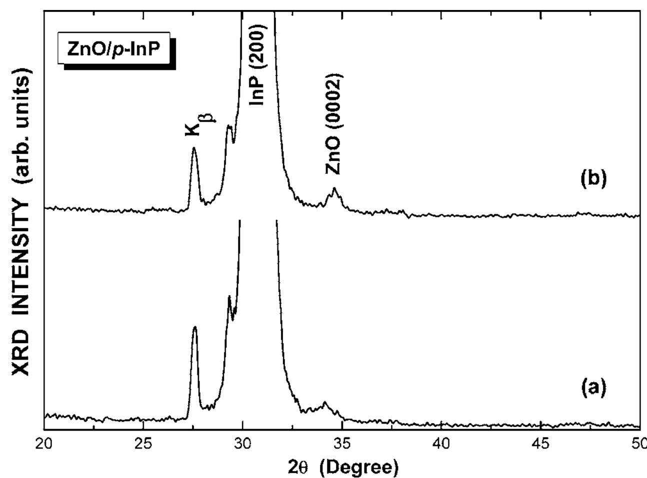

FIG. 1. XRD patterns of the (a) as-grown and (b) annealed ZnO thin films grown on p-InP (100) substrates.

mately 30 μm and then argon-ion milling at liquid-nitrogen temperature to electron transparency. The AFM measurements were performed by using a model SPA400 system (Seiko Instruments Inc., Tokyo, Japan) in the contact mode.

Figure 1 shows XRD patterns for the (a) as-grown and (b) annealed ZnO films grown on p-InP (100) substrates. The (0002) $K\alpha_1$ diffraction peak corresponding to the ZnO film together with the (200) $K\alpha_1$ diffraction peak corresponding to the InP (100) substrate, is observed. Because the thickness of the ZnO films is very thin, the intensity of the (0002) $K\alpha_1$ diffraction peak corresponding to the ZnO films is very small in comparison with that of the (200) $K\alpha_1$ diffraction peak corresponding to the InP (100) substrate. The XRD patterns indicate that the as-grown and the annealed ZnO films grown on the InP (100) substrates have a c-axis orientation that gives the lowest surface free energy.[20]

Figures 2(a) and 2(c) show cross-sectional bright-field TEM images of the as-grown and annealed ZnO thin films grown on p-InP substrates, and Figs. 2(b) and 2(d) show the corresponding cross-sectional HRTEM images. The $\{01\bar{1}2\}$ facet planes with high-order-indexed unstable planes in the ZnO thin films seen in Fig. 2(b) appear at the surface of the as-grown ZnO thin film because the diffusion rate of the atoms on the ZnO surface during the columnar growth is smaller than their deposition rate.[21] Therefore, the surface of the ZnO columns is unstable because the ZnO surface main-

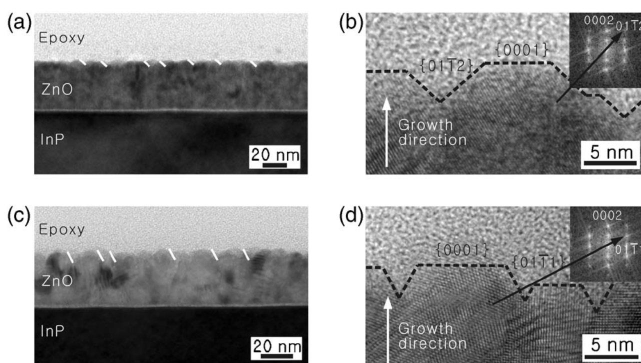

FIG. 2. Cross-sectional bright-field TEM images of the (a) as-grown and the (c) annealed ZnO thin films grown on p-InP (100) substrates. (b) and (d) are high-resolution TEM images for top regions of the as-grown and the annealed ZnO thin films grown on p-InP (100) substrates. The inserts of (b) and (d) are fast-Fourier-transformed diffraction patterns of the as-grown and annealed ZnO thin films grown on p-InP (100) substrates.

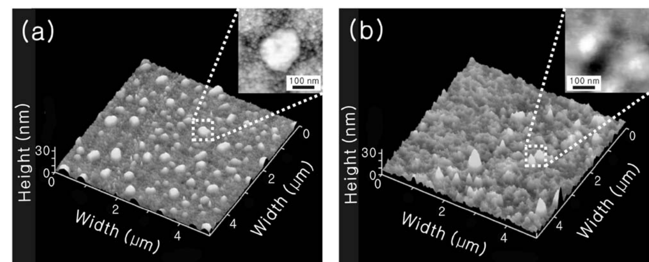

FIG. 3. AFM images of the (a) as-grown and (b) annealed ZnO thin films grown on p-InP (100) substrates. The inserts are magnified images for subpopulations of the as-grown and annealed ZnO grains.

tains a convex shape.[22] The $\{01\bar{1}2\}$ facet planes with high-order-indexed unstable planes in the ZnO grains with a size of about 10 nm, as seen in Fig. 2(b), are transformed into more stable $\{01\bar{1}1\}$ facet planes in the ZnO grains with a size of about 12 nm, as seen in Fig. 2(d), to become stabilized as $\{01\bar{1}0\}$ planes,[23] because the energy of the grain boundary is less than those of the two neighboring surfaces.[22] Therefore, the side surfaces of the ZnO grains become parallel to the direction of grain growth by diffusing unstable atoms in high-ordered facet planes to the vicinity of grain boundaries during thermal treatments.

The surface morphologies of (a) as-grown and (b) annealed ZnO thin films grown on p-InP (100) substrates, as determined from the AFM measurements, are shown in Fig. 3. The root mean squares of the average-surface roughnesses of the as-grown and annealed ZnO thin films are 1.730 and 3.121 nm, respectively. Because the surface morphology of the ZnO films at an initial stage of thermal annealing becomes very rough due to the grain growth resulting from the reduction of the boundaries between the grains, the annealed ZnO films show only a very small amount of high protrusions. The magnified AFM images seen in the inserts in Fig. 3 indicate that several ZnO grains with similar height and growth direction constitute the subpopulations with a size of about 180 nm consisting of 18 and 15 ZnO grains for as-grown and annealed ZnO thin films, respectively, to reduce the interface energy between ZnO grains.[17] Therefore, the surface morphology of ZnO thin films is determined by the surface curvatures of subpopulations fixed by the side surfaces of ZnO grains.

Schematic diagrams for the surface evolution of the subpopulation morphology in the early stage of thermal annealing of ZnO thin films grown on p-InP substrates are shown in Fig. 4. During the initial growth stage of the ZnO thin film, the nucleus growth process for ZnO induces impingement and coalescence between ZnO islands, resulting in the formation of a columnar structure of ZnO grains with the surfaces of a convex shape. During impingement and coalescence between ZnO islands, several ZnO grains with similar height and growth direction constitute the subpopulations to reduce the interface energy between ZnO grains, as shown in Fig. 4(a).[17] The surface morphology of ZnO thin films is determined by surface curvature of subpopulations fixed by the side surfaces of ZnO grains. During thermal annealing, the unstable atoms with high-ordered facet planes diffuse in the vicinity of the grain boundaries to reduce the surface energy because the energy of the grain boundary is less than those of the two neighboring surfaces.[22] The grain boundary becomes parallel to the direction of grain growth, as shown in Fig. 4(b). Therefore, the surface curvature of subpopula-

Downloaded 22 Apr 2013 to 143.248.118.122. This article is copyrighted as indicated in the abstract. Reuse of AIP content is subject to the terms at: http://apl.aip.org/about/rights_and_permissions

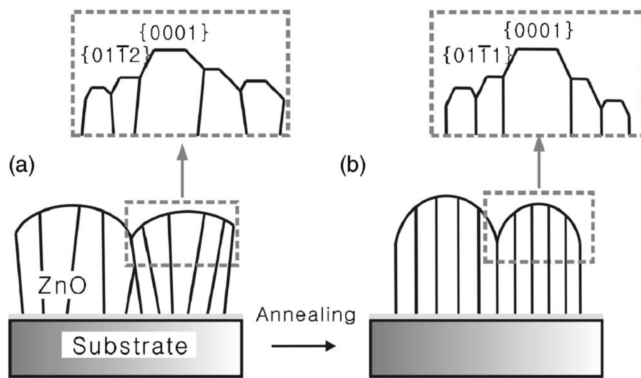

FIG. 4. Schematic cross-sectional diagrams for the surface curvatures in subpopulations consisting of ZnO grains for (a) the as-grown and (b) annealed ZnO thin films grown on the *p*-InP (100) substrates.

tions of ZnO grains became sharp in the early stage of thermal annealing.

In summary, the TEM and the HRTEM images showed that the columnar structure and the surface morphology of ZnO grains became stabilized due to thermal annealing. The surface curvature of the subpopulations consisting of several ZnO grains became sharp because the side surfaces of the ZnO grains became parallel to the direction of grain growth. Therefore, the AFM images showed that while the top surface of the ZnO grains became flat, the surface morphology of the ZnO thin films determined by the curvature of the subpopulations consisting of ZnO grains was deteriorated in the early stage of thermal annealing.

This work was supported by the Korea Science and Engineering Foundation (KOSEF) grant funded by the Korea government (MEST) (No. R0A-2007-000-20044-0).

[1] R. F. Service, Science **276**, 895 (1997).
[2] Z. W. Pan, Z. R. Dai, and Z. L. Wang, Science **291**, 1947 (2001).
[3] D. M. Bagnall, Y. Chen, Z. Zhu, T. Yao, S. Koyama, M. Y. Shen, and T. Goto, Appl. Phys. Lett. **70**, 2230 (1997).
[4] Z. K. Tang, G. K. L. Wong, P. Tu, M. Kawasaki, A. Ohtomo, H. Koinuma, and Y. Segawa, Appl. Phys. Lett. **72**, 3270 (1998).
[5] T. Soki, Y. Hatanaka, and D. C. Look, Appl. Phys. Lett. **76**, 3257 (2000).
[6] S.-K. Kim, S.-Y. Jeong, and C.-R. Cho, Appl. Phys. Lett. **82**, 562 (2003).
[7] H. S. Lee, J. Y. Lee, T. W. Kim, and M. D. Kim, J. Appl. Phys. **94**, 6354 (2003).
[8] B. Yaglioglu, H.-Y. Yeom, and D. C. Paine, Appl. Phys. Lett. **86**, 261908 (2005).
[9] K. Ogata, S.-W. Kim, Sz. Fujita, and Sg. Fujita, J. Cryst. Growth **240**, 112 (2002).
[10] Y. L. Liu, Y. C. Liu, Y. X. Liu, D. Z. Shen, Y. M. Lu, J. Y. Zhang, and X. W. Fan, Physica B **322**, 31 (2002).
[11] J. W. Shin, J. Y. Lee, Y. S. No, T. W. Kim, and W. K. Choi, Appl. Phys. Lett. **89**, 101904 (2006).
[12] J. M. Yuk, J. Y. Lee, J. H. Jung, T. W. Kim, D. I. Son, and W. K. Choi, Appl. Phys. Lett. **90**, 031907 (2007).
[13] M. K. Ryu, S. H. Lee, M. S. Jang, G. N. Panin, and T. W. Kang, J. Appl. Phys. **92**, 154 (2002).
[14] E. S. Shim, H. S. Kang, S. S. Pang, J. S. Kang, I. Yun, and S. Y. Lee, Mater. Sci. Eng., B **102**, 366 (2003).
[15] J. J. Lee, Y. B. Kim, and Y. S. Yoon, Appl. Surf. Sci. **244**, 365 (2005).
[16] I. W. Kim, S. J. Doh, C. C. Kim, J. H. Je, J. Tashiro, and M. Yoshimoto, Appl. Surf. Sci. **241**, 179 (2005).
[17] C. V. Thompson, Annu. Rev. Mater. Sci. **30**, 159 (2000).
[18] Y. Yoshino, K. Inoue, M. Takeuchi, T. Makino, Y. Katayama, and T. Hata, Vacuum **59**, 403 (2000).
[19] X. Xu, C. Guo, Z. Qi, H. Liu, J. Xu, C. Shi, C. Chong, W. Huang, Y. Zhou, and C. Xu, Chem. Phys. Lett. **364**, 57 (2002).
[20] N. Fujimura, T. Nishhara, S. Goto, J. Xua, and T. Ito, J. Cryst. Growth **130**, 269 (1993).
[21] J. W. Shin, J. Y. Lee, T. W. Kim, Y. S. No, W. J. Cho, and W. K. Choi, Appl. Phys. Lett. **88**, 091911 (2006).
[22] W. D. Nix and B. M. Clemens, J. Mater. Res. **12**, 3467 (1999).
[23] N. Boukos, C. Chandrinou, C. Stogios, K. Giannakopoulos, and A. Travlos, Nanotechnology **18**, 275601 (2007).

Downloaded 22 Apr 2013 to 143.248.118.122. This article is copyrighted as indicated in the abstract. Reuse of AIP content is subject to the terms at: http://apl.aip.org/about/rights_and_permissions